

PCCP

Accepted Manuscript



This is an *Accepted Manuscript*, which has been through the Royal Society of Chemistry peer review process and has been accepted for publication.

Accepted Manuscripts are published online shortly after acceptance, before technical editing, formatting and proof reading. Using this free service, authors can make their results available to the community, in citable form, before we publish the edited article. We will replace this *Accepted Manuscript* with the edited and formatted *Advance Article* as soon as it is available.

You can find more information about *Accepted Manuscripts* in the [Information for Authors](#).

Please note that technical editing may introduce minor changes to the text and/or graphics, which may alter content. The journal's standard [Terms & Conditions](#) and the [Ethical guidelines](#) still apply. In no event shall the Royal Society of Chemistry be held responsible for any errors or omissions in this *Accepted Manuscript* or any consequences arising from the use of any information it contains.

Significant enhancement of photocatalytic activity of rutile TiO₂ compared with anatase TiO₂ upon Pt nanoparticle deposition studied by far-ultraviolet spectroscopy[†]

Cite this: DOI: 10.1039/x0xx00000x

Received 00th January 2012,
Accepted 00th January 2012

DOI: 10.1039/x0xx00000x

www.rsc.org/

Ichiro Tanabe,* Takayuki Ryoki and Yukihiro Ozaki*

Absorption spectra of anatase and rutile TiO₂ in the 150–300-nm region before and after the deposition of Pt nanoparticles were measured. For anatase TiO₂, the spectral intensity in the longer wavelength region decreased (> ~210 nm), while that in the shorter wavelength region increased (< ~210 nm). In particular, spectral band intensity in far-ultraviolet (FUV) region (~160 nm) was increased. In contrast, the spectral intensity of rutile TiO₂ increased over the entire wavelength region under investigation. Rutile TiO₂ showed spectral band at a longer wavelength region (~170 nm) than anatase TiO₂, and the difference in the band wavelengths in the FUV region was due to the differences in the electronic structures of their phase. The decrease and increase in the intensity upon the Pt nanoparticle deposition suggests electron transfer from the TiO₂ to Pt nanoparticles and enhancement of charge-separation, respectively. The photocatalytic activity of rutile TiO₂, as evaluated by a photo-degradation reaction of methylene blue, increased more than that of anatase TiO₂ upon the deposition of Pt nanoparticles. Thus, we concluded that the charge-separation efficiency of rutile TiO₂ is enhanced relative to that of anatase TiO₂ upon the deposition of Pt nanoparticles.

Introduction

Titanium dioxide (TiO₂) is one of the most attractive materials with applications in a wide range of fields,^{1–6} particularly in photocatalysis^{1–3} and next-generation solar cell materials.^{4–6} Two types of readily available varieties of crystalline TiO₂, anatase and rutile, exhibit different chemical, physical, optical, and photocatalytic properties.^{7–9} The band-gap energy of anatase TiO₂ (~3.2 eV) is higher than that of rutile TiO₂ (~3.0 eV),⁸ the reflectance spectra of anatase and rutile TiO₂ in the near-ultraviolet (NUV, 200–400 nm) region have also been reported.⁹ However, until quite recently, it was difficult to measure the optical properties of TiO₂ in the far-ultraviolet (FUV, 140–200 nm) region because of very intense absorption (absorbance index $\alpha > 10^7 \text{ cm}^{-1}$),¹⁰ thus, it was not possible to clarify the differences in the optical properties of anatase and rutile TiO₂ based on the FUV region, despite the fact that this region provides substantial information about the electronic states of various materials.^{11–13} TiO₂ is activated upon irradiation with NUV-FUV light (<390 nm for anatase phase, <410 nm for rutile phase), and therefore, exploration of optical properties in both the NUV and FUV regions is highly important.

TiO₂ containing metal nanoparticles have also been extensively investigated in recent decades by many research groups.^{8,14–20} Loading TiO₂ with metal (such as Pt, Pd, and Au) nanoparticles increases the photocatalytic activity of TiO₂.^{14–16} However, it is difficult to systematically estimate the effects of

these surface modifications on TiO₂ electronic states in the FUV–NUV region. Therefore, the differences in the electronic state and photocatalytic activity between anatase and rutile TiO₂ upon surface modifications such as metal nanoparticle deposition are not well understood. Because the ability to measure these differences by a simple and systematic method is important for material design, we have recently measured the FUV–NUV (150–300 nm) spectra of TiO₂ and metal (Pt, Pd, and Au)-modified TiO₂, and found that the deposition of metal nanoparticles alters the spectral shape and intensity. Upon the deposition of metal nanoparticles, intensity in the longer wavelength region decreases, while that in the shorter wavelength region increases. The former reflects the transfer of electrons from TiO₂ to metals, and the latter indicates enhancement of charge-separation efficiency.²¹ Moreover, there is a strong positive relationship between the degree of spectral changes, photocatalytic activities, and the work function of the deposited metals.²¹ To measure the spectra (including the FUV region), we employed our original FUV spectrometer that is based on attenuated total reflection (ATR),^{11–13} which enables us to measure the spectra of liquid and solid samples such as water,^{11,12} aqueous solutions,^{22,23} and organic molecules^{24–26} in the 140–300 nm region.

In this study, the ATR–FUV spectra of anatase and rutile TiO₂ particles with 5- μm secondary particle diameter, 200- and 40-nm diameters, respectively, were measured. Subsequently, the ATR–FUV spectra of TiO₂ with Pt nanoparticles were also obtained, and the spectral changes and photocatalytic activities

of all TiO₂ species were investigated. The anatase TiO₂ particles showed a broad feature at ~160 nm. Upon the deposition of Pt nanoparticles, the intensity of the spectrum in the region containing this band (150–180 nm) increased, while the intensity in the longer wavelength region (240–300 nm) decreased. In contrast, for the rutile TiO₂ particles, the intensity increased over the entire measured region (150–300 nm) upon the deposition of Pt nanoparticles, and the spectrum showed a band at a longer wavelength region (~170 nm) than anatase TiO₂. The differences in band wavelength in the FUV region are due to differences in the electronic structure of anatase and rutile TiO₂. The increase over the entire region of rutile TiO₂ upon the deposition of Pt nanoparticles indicates that the enhancement of the charge-separation efficiency of rutile TiO₂ is larger than that of anatase TiO₂. The photocatalytic activities of the rutile TiO₂ particles were more enhanced by the deposition of Pt nanoparticles than those of the anatase TiO₂ particles. In this way, we have revealed the differences in the electronic states of anatase and rutile phase TiO₂, and how they change upon the deposition of Pt nanoparticles, which is strongly related to their photocatalytic activities.

Experimental

Anatase and rutile TiO₂ (5- μ m secondary particle diameter) were purchased from Wako Pure Chemical Industries, Ltd. Anatase TiO₂ (200- and 40-nm diameters) and rutile TiO₂ (40-nm diameter) were purchased from Ishihara Sangyo Kaisya Industries, Ltd., while rutile TiO₂ (200 nm) was purchased from Toho Titanium Company, Ltd. All varieties of anatase and rutile TiO₂ particles were used as purchased. Pt nanoparticle colloids (10 mM, water and ethanol solvent, 1–6-nm diameter, protected by polyvinylpyrrolidone) were purchased from Wako Pure Chemical Industries, Ltd. During the ATR-FUV measurement, the samples were placed on a sapphire internal reflection element (IRE), and the ATR spectra were measured using an evanescent wave as a probe light.

TiO₂ (1 g) and metal colloids (200 μ L) were mixed in an agate mortar until the solvent completely evaporated off to the atmosphere. TiO₂ particles with and without Pt nanoparticles were placed on the sapphire IRE, and the FUV-NUV spectra were measured using an ATR-FUV spectrometer. In the FUV region, both H₂O and O₂ present in the atmosphere yield very intense absorptions, and thus the spectrometer must be purged with N₂ gas. The ATR-FUV system employed in this study used a 30-W deuterium lamp as a light source. SEM images were observed by model S-5000 (Hitachi Ltd., Tokyo, Japan), operated at 20 kV.

Methylene blue was purchased from Wako Pure Chemical Industries, Ltd. A Hg-Xe lamp (Luminar Ace LA-300UV, Hayashi Watch Works) equipped with a UV-pass filter (Wavelength = 300–350 nm, UTVAF-50S-34U, CVI Laser, LLC) was used as the UV light source. An aqueous solution of methylene blue (20 μ M, 20 mL) was mixed with TiO₂ only and TiO₂-Pt powder (5 mg) using a magnetic stirrer, followed by UV irradiation (~10 μ W cm⁻²) for 30 min. After the irradiation, TiO₂ was separated from the solution by centrifugation (15,000 rpm, 1 min). The absorption spectra of the methylene blue aqueous solutions were measured both before and after UV irradiation.

Results and discussion

ATR-FUV-NUV spectra of anatase and rutile TiO₂

ATR-FUV-NUV spectra in the 150–300 nm wavelength region of commercial anatase and rutile TiO₂ particles with 5- μ m secondary particle diameter, and 200- and 40-nm diameter, respectively, were measured. The spectra of the anatase TiO₂ particles showed a broad band at ~160 nm independent of the particle size, which, as previously reported, was assigned to the $t_{2g}(\pi) \rightarrow e_g(\sigma^*)$ transition (Fig. 1a).²¹ On the other hand, the spectral intensities of rutile TiO₂ particles were lower than those of anatase TiO₂ (Fig. 1b), and the spectra showed no defined peak in the FUV region. Fig. 2a–h shows the SEM images of TiO₂ particles. Commercial TiO₂ nanoparticles have definite diameters for both the anatase and rutile phases (200 and 40 nm, respectively); however, for TiO₂ particles with 5- μ m secondary particle diameters, the original particle diameters of the anatase and rutile phases vary by several dozen and several hundred nanometers, respectively. In actuality, the intensity of the FUV-NUV spectrum of anatase TiO₂ with 5- μ m secondary particle diameter is close to that of anatase TiO₂

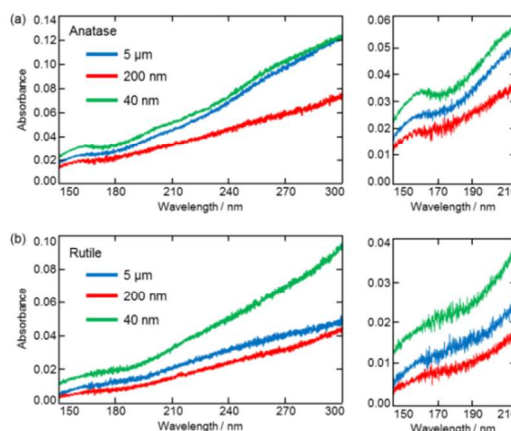


Fig. 1 ATR-FUV-NUV spectra of (a) anatase and (b) rutile TiO₂ particles with (blue) 5- μ m, (red) 200-nm, and (green) 40-nm diameters.

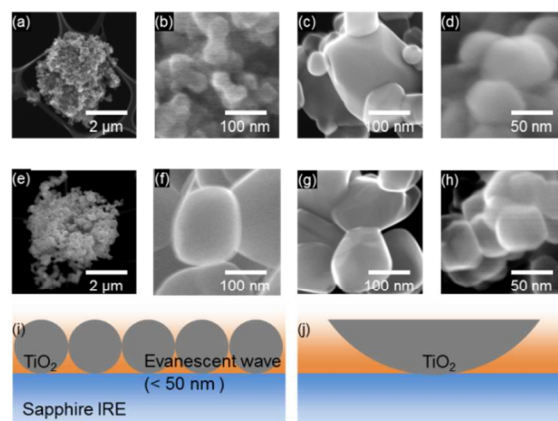


Fig. 2 (a–h) SEM images of (a–d) anatase and (e–h) rutile TiO₂ particles with (a, b, e, f) 5- μ m, (c, g) 200-nm, and (d, h) 40-nm diameters. (i, j) Measurement mechanism of TiO₂ using ATR-FUV spectrometer for (i) 40-nm and (j) 5- μ m diameter TiO₂.

with 40-nm particle diameter (Fig. 1a). Likewise, the intensity of rutile TiO₂ with 5- μ m secondary particle diameter is close to that of rutile TiO₂ with 200-nm particle diameter (Fig. 1b). These results show that the intensity of the TiO₂ spectra is largely dependent on particle size. This is because the amount of TiO₂ with 40-nm diameter particles in the evanescent wave range (Fig. 2i) is larger than the amount of TiO₂ with 200-nm diameter particles (Fig. 2j). Actually, calculated occupancies of 40-nm and 200-nm diameters spheres in the evanescent wave range (penetration depth = 50 nm) are approximately 63% and 32%, respectively. On the other hand, integrated intensity ratios of absorbance of 40-nm diameter TiO₂ to that of 200-nm diameter TiO₂ are \sim 1.7 (for Fig. 1a) or \sim 2.3 (for Fig. 1b), which are corresponding with the occupancies.

Spectral changes of anatase and rutile TiO₂ upon Pt nanoparticles deposition

The ATR-FUV-NUV spectra of TiO₂ modified with Pt nanoparticles were also measured. The Pt nanoparticles (1–6-nm diameter) were deposited by mixing TiO₂ particles (1 g) with commercially available Pt nanoparticle colloids (200 μ L, 10 mM in water/ethanol solution, protected with polyvinylpyrrolidone (PVP), Wako Pure Chemical Industrial, Ltd.) in an agate mortar until the solvent completely evaporated off to the atmosphere. A typical SEM image of the TiO₂-Pt nanoparticles is shown in Fig. S1. Fig. 3a–f shows a comparison of the ATR-FUV spectra of TiO₂-Pt nanoparticles (red lines) with that of TiO₂ only (black lines). It is noted that PVP has no substantial effect on the ATR-FUV spectra as shown in our previous paper.²¹ The ATR-FUV spectra of rutile TiO₂ particles modified with Pt nanoparticles have bands at \sim 170 nm, while the spectra of anatase TiO₂ particles have bands

at \sim 160 nm. The difference in the band wavelengths in the FUV region is due to the differences in the electronic structures of the anatase and rutile phases, as previous calculations have shown.²⁷ The spectral differences between the anatase and rutile phases in the NUV (>200 nm) region have also been previously reported,⁹ and the band wavelengths of rutile-phase TiO₂ are longer than those of anatase-phase TiO₂. By employing an ATR-FUV spectrometer, we can, for the first time, compare the optical spectra of anatase and rutile TiO₂ in the FUV region.

For anatase TiO₂ particles (Fig. 3a–c), the spectral intensity in the longer wavelength region decreases, while that in the shorter wavelength region increases upon the deposition of Pt nanoparticles. As we have previously reported,²¹ the decrease in the intensity in the longer wavelength region is due to charge transfer at the TiO₂-Pt interface, and the increase in the shorter wavelength region is due to the enhancement of the charge-separation efficiency upon the deposition of Pt nanoparticles. The work function of TiO₂ (\sim 4.0 eV for anatase-phase TiO₂) is smaller than that of Pt (\sim 5.7 eV).¹⁶ Therefore, when TiO₂ contacts the Pt nanoparticles, electrons in TiO₂ inflow to the Pt nanoparticles until both the Fermi levels are equalized.¹ As a result, the number of electrons in relatively high-energy levels (*i.e.*, electrons that can be excited at a relatively longer wavelength) is decreased, resulting in the suppression of spectral intensity in the longer wavelength region. In contrast, Pt nanoparticles on TiO₂ can act as a sink for photo-excited electrons,^{18,19} resulting in the enhancement of the charge-separation efficiency, and an increase in the spectral intensity in the shorter wavelength region. This enhancement process may also occur in the longer wavelength region; however, the total change in the spectral intensity is affected by this enhancement as well as by the decrease in the number of electrons upon contact between TiO₂ and Pt nanoparticles.²¹

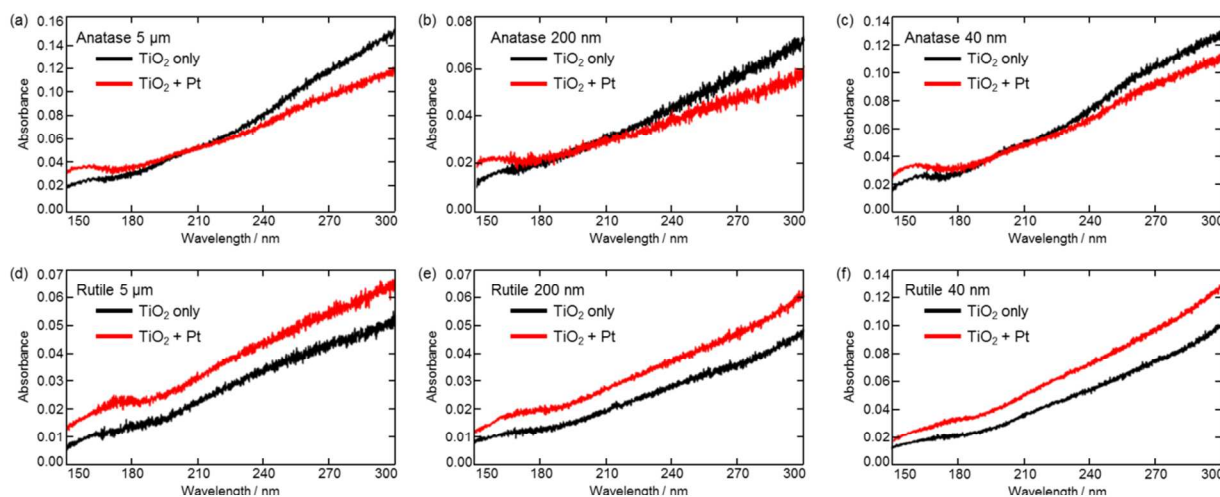


Fig. 3 ATR-FUV-NUV spectra of (a–c) anatase and (d–f) rutile TiO₂ particles with (a, d) 5- μ m, (b, e) 200-nm, and (c, f) 40-nm diameters, before (black) and after (red) the deposition of Pt nanoparticles.

In contrast, the spectral intensity of rutile TiO₂ nanoparticles (Fig. 3d–f) increases over the entire region upon the deposition of Pt nanoparticles. When the anatase TiO₂ is modified with Au nanoparticles, the intensity in the longer wavelength region decreases, as it does for the anatase TiO₂-Pt nanoparticles based on the electron transfer described above.²¹ The work function of Au (\sim 4.7 eV) is approximately 1.0 eV lower than

that of Pt, while that of rutile TiO₂ is 0.2 eV lower than that of anatase TiO₂ (at most).^{7,8} Therefore, if the magnitude of the effect of charge-separation enhancement for rutile TiO₂ is the same as that for anatase TiO₂, the intensity in the longer wavelength region should decrease. However, in practice, the spectral intensity of rutile TiO₂ increases even in the longer wavelength region. Herein, it is important that the increase of

ATR-FUV intensity means the enhancement of charge-separation as mentioned above. Therefore, these results indicate that the magnitude of the effect of charge-separation enhancement for rutile TiO₂ is higher than it is for anatase TiO₂. Subsequently, we estimated their photocatalytic activities in order to value the enhancement of the charge-separation efficiency upon the Pt nanoparticles deposition.

Enhancement of photocatalytic activities of anatase and rutile TiO₂ upon Pt nanoparticles deposition

Photocatalytic activities of TiO₂ particles with and without Pt nanoparticles were estimated using a photo-degradation reaction of methylene blue. A methylene blue aqueous solution (20 μM, 20 mL), including TiO₂ particles with and without Pt nanoparticles (5 mg), was irradiated with UV light (300–350 nm, ~10 μW cm⁻²) for 30 min, and the absorption spectra before and after UV irradiation were measured (Fig. S2). The photocatalytic activity of each sample was estimated by Equation (1), where I_0 and I represent the absorbance values at 665 nm before and after the photo-degradation reaction, respectively.

$$\text{Photocatalytic activity} = 1 - I/I_0 \quad (1)$$

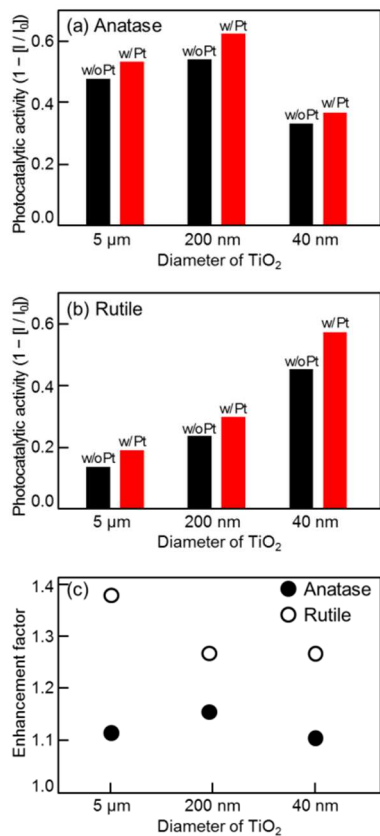


Fig. 4 Photocatalytic activities ($1 - I/I_0$) of (a) anatase and (b) rutile TiO₂ particles (black) before and (red) after the deposition of Pt nanoparticles. (c) Enhancement factors of (filled circle) anatase and (open circle) rutile TiO₂ particles. TiO₂ particle diameters are 5 μm, 200 nm, and 40 nm.

Fig. 4a (anatase TiO₂) and 4b (rutile TiO₂) show the plots of the photocatalytic activities of TiO₂ (black) and TiO₂ with Pt nanoparticles (red) as a function of particle diameter. For 5-μm secondary particle diameter and 200-nm diameter TiO₂ particles, the photocatalytic activity of anatase TiO₂ is higher

than that of rutile TiO₂ of the same size, which is in agreement with previous reports.³ For rutile TiO₂, the smaller TiO₂ particle shows larger photocatalytic activity, and TiO₂ with 5-μm secondary diameter shows the smallest photocatalytic activity. These results are obtained because the smaller particle has the larger surface area.²⁸

The anatase TiO₂ particles with 40-nm diameters show exceptionally low photocatalytic activity. This is likely because the synthesis of small anatase TiO₂ nanoparticles require lower temperatures than large anatase particles and rutile particles do,²⁹ as well as because anatase TiO₂ particles with 40-nm diameters have more lattice defects that decrease the photocatalytic activity.³⁰ The photocatalytic activities of all TiO₂ nanoparticles are enhanced upon the deposition of Pt nanoparticles. The photocatalytic activities of anatase TiO₂ were 0.47, 0.53, and 0.33 (5-μm, 200-nm, and 40-nm diameter particles, respectively), and increased to 0.52, 0.62, and 0.36 upon the deposition of Pt nanoparticles. For rutile TiO₂, the photocatalytic activities were 0.13, 0.23, and 0.44 (5-μm, 200-nm, and 40-nm diameter particles, respectively), and increased to 0.18, 0.28, and 0.55. The ratios of the photocatalytic activity of TiO₂ modified with Pt nanoparticles to that of TiO₂ only were calculated as an “enhancement factor”^{31,32} for each TiO₂ particle. As shown in Fig. 4c, the rutile TiO₂ particles (open circles) show higher enhancement of their photocatalytic activity than anatase TiO₂ particles (filled circles). Many research groups have reported that the photocatalytic activity of TiO₂ is improved upon the deposition of metal nanoparticles.^{14–20,33} However, most of these groups have focused on either only anatase TiO₂ or a mixture of anatase and rutile TiO₂,^{14–20} because both bare anatase and a mixture of anatase and rutile TiO₂ show higher photocatalytic activity than bare rutile TiO₂ does in many reactions. Rutile TiO₂ has been used primarily for deliberations of reactive mechanisms. For example, Li and co-workers revealed that the (110) surface of rutile TiO₂ was more selectively deposited with Pt nanoparticles compared with the (001) surface, and that the photocatalytic activity was improved by Pt deposition.³³ However, there are no literature reports involving the comparison of anatase and rutile TiO₂ in terms of their optical and/or photocatalytic property changes upon the deposition of metal. In the study herein, we have systematically compared the electronic state changes and photocatalytic activity of anatase and rutile TiO₂, and have shown, on the basis of ATR-FUV-NUV spectral measurements and estimations of photo-degradation reaction activity, that the enhancement of charge-separation efficiency upon the deposition of Pt nanoparticles for rutile TiO₂ is higher than that for anatase TiO₂.

Conclusions

In summary, the absorption spectra of anatase and rutile TiO₂ particles (with 5-μm, 200-nm, and 40-nm diameters) with and without Pt nanoparticles were measured in the FUV-NUV (150–300 nm) region. The intensity of the anatase TiO₂ spectrum decreased in the longer wavelength region and increased in the shorter wavelength region, which indicates the transfer of electrons from TiO₂ to the Pt nanoparticles and the enhancement of charge separation, respectively. On the other hand, for rutile TiO₂, the spectral intensity increased over both wavelength regions, indicating that the effect of the enhancement of charge separation is larger than the effect of the transferred electron. The measurements of the photocatalytic activities also showed that rutile TiO₂ showed greater enhancement than did anatase TiO₂. These results show that the

photocatalytic activity of rutile TiO₂ is more enhanced than that of anatase TiO₂ upon the deposition of Pt nanoparticles, and also demonstrates that the corresponding changes in the electronic states can be estimated by facile and systematic ATR–FUV–NUV spectral measurements. When designing TiO₂-based materials, it is important to have an insight regarding the enhancement of the charge-separation efficiency, which depends on the nature of the crystalline structure. This can allow for the elucidation of the enhancement mechanism, and lead to the development of high-efficiency optical materials such as photocatalysts and solar cells.

Acknowledgements

This work was supported by the MEXT-Supported Program of the Strategic Research Foundation at Private University (2012–2016), The Sumitomo Foundation, and Izumi Science and Technology Foundation. We are grateful to Dr. K. Tawa (National Institute of Advanced Industrial Science and Technology) for helpful discussions.

Notes and references

Department of Chemistry, School of Science and Technology, Kwasei Gakuin University, Gakuen 2-1, Sanda, Hyogo, Japan, E-mail: i-tanabe@kwasei.ac.jp (for IT), ozaki@kwasei.ac.jp (for YO)

† Electronic Supplementary Information (ESI) available: Fig. S1 and S2. See DOI: 10.1039/b000000x/

- 1 A. L. Linsebigler, G. Lu, J. T. Yates Jr., *Chem. Rev.*, 1995, **95**, 735.
- 2 X. Chen, S. S. Mao, *Chem. Rev.*, 2007, **107**, 2891.
- 3 M. R. Hoffmann, S. T. Martin, W. Choi, D. W. Bahnemann, *Chem. Rev.*, 1995, **95**, 69.
- 4 B. O'Regan, M. Grätzel, *Nature*, 1991, **353**, 737.
- 5 M. K. Nazeeruddin, P. Péchy, T. Renouard, S. M. Zakeeruddin, R. Humphry-Baker, P. Comte, P. Liska, L. Cevey, E. Costa, V. Shklover, L. Spiccia, G. B. Deacon, C. A. Bignozzi, M. Grätzel, *J. Am. Chem. Soc.*, 2001, **123**, 1613.
- 6 P. V. Kamat, *J. Phys. Chem. C*, 2008, **112**, 18737.
- 7 K. Tanaka, M. F.V. Capule, T. Hisanaga, *Chem. Phys. Lett.*, 1991, **187**, 73.
- 8 U. Diebold, *Sur. Sci. Rep.*, 2003, **48**, 53.
- 9 J. Zhang, M. Li, Z. Feng, J. Chen, C. Li, *J. Phys. Chem. B*, 2006, **110**, 927.
- 10 G. E. Jellison Jr., L. A. Boatner, J. D. Budai, B.-S. Jeong, D. P. Norton, *J. Appl. Phys.*, 2003, **93**, 9537.
- 11 N. Higashi, A. Ikehata, Y. Ozaki, *Rev. Sci. Instrum.*, 2007, **78**, 103107.
- 12 Y. Ozaki, Y. Morisawa, A. Ikehata, N. Higashi, *Appl. Spectrosc.*, 2012, **66**, 1.
- 13 T. Morisawa, N. Higashi, K. Takaba, Y. Kariyama, N. Goto, A. Ikehata, Y. Ozaki, *Rev. Sci. Instrum.*, 2012, **83**, 073103.
- 14 B. Kraeutler, A. J. Bard, *J. Am. Chem. Soc.*, 1978, **100**, 2239.
- 15 T. Kawai, T. Sakata, *Nature*, 1979, **282**, 283.
- 16 Y. Nosaka, K. Norimatsu, H. Miyama, *Chem. Phys. Lett.*, 1984, **106**, 128.
- 17 Y. Tian, T. Tatsuma, *Chem. Commun.*, 2004, 1810.
- 18 M. Jakob, H. Levanon, P. V. Kamat, *Nano Lett.*, 2003, **3**, 353.
- 19 M. Murdoch, G. I. N. Waterhouse, M. A. Nadeem, J. B. Metson, M. A. Keane, R. F. Howe, J. Llorca, H. Idriss, *Nature Chem.*, 2011, **3**, 489.
- 20 P. V. Kamat, *J. Phys. Chem. Lett.*, 2012, **3**, 663.
- 21 I. Tanabe, Y. Ozaki, *Chem. Commun.*, 2014, **50**, 2117.
- 22 A. Ikehata, M. Mitsuoka, Y. Morisawa, N. Kariyama, N. Higashi, Y. Ozaki, *J. Phys. Chem. A*, 2010, **114**, 8319.
- 23 T. Goto, A. Ikehata, Y. Morisawa, N. Higashi, Y. Ozaki, *Phys. Chem. Chem. Phys.*, 2012, **14**, 8097.
- 24 Y. Morisawa, A. Ikehata, N. Higashi, Y. Ozaki, *Chem. Phys. Lett.*, 2009, **476**, 205.
- 25 S. Tachibana, Y. Morisawa, A. Ikehata, H. Sato, N. Higashi, Y. Ozaki, *Appl. Spectrosc.*, 2011, **65**, 221.
- 26 Y. Morisawa, A. Ikehata, N. Higashi, Y. Ozaki, *J. Phys. Chem. A*, 2011, **115**, 562.
- 27 M. Landmann, E. Rauls, W. G. Schmidt, *J. Phys.: Condens. Matter*, 2012, **24**, 195503.
- 28 N. Xu, Z. Shi, Y. Fan, J. Dong, J. Shi, M. Z.-C. Hu, *Ind. Eng. Chem. Res.*, 1999, **38**, 373.
- 29 Q. Zhang, L. Gao, J. Guo, *J. Eur. Ceram. Soc.*, 2000, **20**, 2153.
- 30 S. Ikeda, N. Sugiyama, S. Murakami, H. Kominami, Y. Kera, H. Noguchi, K. Uosaki, T. Torimoto, B. Ohtani, *Phys. Chem. Chem. Phys.*, 2003, **5**, 778.
- 31 J. I. L. Chen, G. von Freymann, V. Kitaev, G. A. Ozin, *J. Am. Chem. Soc.*, 2007, **129**, 1196.
- 32 Z. Zhang, Z. Wang, S.-W. Cao, C. Xue, *J. Phys. Chem. C*, 2013, **117**, 25939.
- 33 J. Zhang, L. Li, T. Yan, G. Li, *J. Phys. Chem. C*, 2011, **115**, 13820.